Sensors & Actuators: B. Chemical 354 (2022) 131198

Contents lists available at ScienceDirect

Sensors and Actuators: B. Chemical

journal homepage: www.elsevier.com/locate/snb

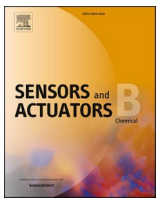

Fabrication of Janus GO/rGO humidity actuator by one-step electrochemical reduction route

Zeriş Aksu [a], Cengiz Han Şahin [b], Murat Alanyalıoğlu [a,c,*]

[a] Atatürk University, Sciences Faculty, Department of Chemistry, 25240 Erzurum, Turkey
[b] Atatürk University, Faculty of Dentistry, 25240 Erzurum, Turkey
[c] Bilecik Şeyh Edebali University, Vocational School, Department of Food Processing, 11230 Bilecik, Turkey

ARTICLE INFO

Keywords:
Humidity actuator
Janus structure
Electrochemical reduction
Graphene oxide paper

ABSTRACT

Graphene oxide (GO) is an insulator and should be converted to reduced graphene oxide (rGO) paper structure by reduction to provide electrochemical activity. This work maintains an essential route to fabricate rGO paper. Hence, the first aim of this study is to produce rGO paper by one-step electrochemical reduction of GO paper by the optimization of quality parameters. Humidity actuators produce mechanical feedback if the moisture is exposed to their surface. To provide this kind of response, Janus materials are good nominated due to their asymmetric surface character in terms of hydrophilicity. GO paper can be performed for this application by converting one side to rGO layers. By this approach, hydrophobic rGO and hydrophilic GO sheets of the Janus system are generated, in which moisture flow swells the GO side and causes bending motion of the material through the rGO layer. In this work, Janus GO/rGO paper has been prepared by one-step electrochemical reduction of one side of the GO paper. Characterization of the samples has been carried out using numerous techniques. Humidity actuator experiments have indicated that Janus GO/rGO paper is acting circularly and there is an exponential relationship between relative humidity and circularly-oriented bending angle of the actuator.

1. Introduction

Graphene has a single carbon atom thick structure with perfect sp^2 hybridization, which is one of the most interesting nanomaterials due to its versatile properties such as flexibility, strength, stability, great surface area, electrical and thermal conductivity. Graphene has taken its place as a basic nanomaterial in many different technological applications since its discovery by mechanical separation in 2004 [1]. Chemical oxidation [2], electrochemical exfoliation [3,4], and chemical vapor deposition [5] are other developed techniques for the production of graphene sheets. Chemical oxidation of graphite results in the formation of graphite oxide. Exfoliation of graphite oxide produces graphene oxide (GO) layers. The most important advantage of GO is its hydrophilic behavior by means of functional groups such as hydroxyl, carbonyl, and epoxy.

Graphene-based paper-like materials are a new era in many applications e.g. supercapacitors [6], batteries [7], electrochemical sensors [8,9], actuators [10], and membranes [11,12] because of adjustment of their many properties such as shape, size, thickness, functionality as far as their high flexibility. GO paper structures have high flexibility. However, the insulator character restricts the usage of electrode material in electrochemical studies. GO papers are generally converted to reduced graphene oxide (rGO) paper using a suitable reduction technique to provide electrical conductivity and/or electrochemical activity. Many different methods are used to prepare rGO paper by direct reduction of GO paper such as thermal annealing [8], chemical reduction [9], photothermal treatment [13], flame-induced process [14], unimpeded liquid permeation [15], supercritical ethanol treatment [16], hydrothermal reduction [12,17]. Another suitable technique is an electrochemical reduction for the production of rGO layers. The electrochemical reduction process can be applied in two-electrode systems, or it can be carried out in a standard three-electrode electrochemical cell at room temperature at an appropriate constant potential or in a controlled manner by potential scanning. Up to now, electrochemical reduction of GO layers has been performed on a suitable substrate e.g. gold [18–20], tin oxide coated glass [21], fluorine-doped tin oxide [22]. This work presents the first time production of rGO paper by direct electrochemical reduction of free-standing GO paper without any

* Corresponding author at: Bilecik Şeyh Edebali University, Vocational School, Department of Food Processing, 11230 Bilecik, Turkey.
E-mail address: murat.alanyalioglu@bilecik.edu.tr (M. Alanyalıoğlu).

https://doi.org/10.1016/j.snb.2021.131198
Received 23 September 2021; Received in revised form 15 November 2021; Accepted 30 November 2021
Available online 2 December 2021

substrate by the optimization of parameters of pH, electroreduction potential, reduction time, and paper thickness.

An actuator is a system that can generate a mechanical response when an appropriate signal is applied. Actuator systems that can act with stimuli such as light [23], heat [24], electrical potential [25], and humidity [26–36] are among important research topics. In humidity actuators, it acts proportionally to the amount of moisture coming to the material surface. Janus structure is generally preferred as a humidity actuator. This kind of behavior is important in energy conversion, artificial muscles, moisture-sensitive switch systems, and quantitative determination of humidity in the environment. Janus GO/rGO paper has extensively been investigated as a humidity actuator because the GO side is hydrophilic, while rGO is relatively hydrophobic [26–36]. For this aim, one side of GO paper has been converted to rGO layers using photo-reduction [28], UV-irradiation [29], laser writing [30], and chemical reduction with Cu [31] or HI [32–35], Al [36].

This study reports the preparation of the Janus GO/rGO structure using controlled electrochemical reduction of one side of flexible GO paper for the first time. In this context, a free-standing GO paper was prepared by vacuum filtration of GO dispersion and then stripped from the membrane. The Janus GO/rGO paper was formed by electrochemical reduction of one side of GO paper using as working electrode in a three-electrode cell under optimum conditions. This Janus GO/rGO paper was tested as a humidity actuator and it exhibited controllable and repeatable mechanical movement proportional to the amount of moisture.

2. Experimental section

All of the purchased reagents beyond this study were of analytical grade and used without further purification. Solutions and dispersions were prepared using Milli-Q ultrapure water (resistivity: 18 MΩ cm^{-1}). GO was synthesized using the modified Hummers method described in our previous publications [8,9,12]. Briefly, graphite powder (Alfa Aesar, 99,99%, 325 mesh) was treated with strong oxidant species of H_2SO_4, $K_2S_2O_8$, P_2O_5, $KMnO_4$, and H_2O_2, respectively. This mixture was dialyzed for 3 weeks to acquire pure graphite oxide. Then, 100 mg of graphite oxide was poured into 100 mL of the aqueous dispersion and left into an ultrasonic bath (Bandelin brand) for 1 h to access 1.0 mg mL^{-1} of GO dispersion.

The production route of the Janus GO/rGO paper has been illustrated in Fig. 1. We have initially fabricated GO paper by vacuum-filtration of 100 mL of GO dispersion through a polycarbonate membrane (Whatman, Ø: 47 mm, pore size: 200 nm). After cleaning it with ultrapure water many times and peeling off from the membrane, free-standing GO paper with a very flexible character is gained. Janus structure was prepared by electrochemical reduction of one side of GO paper at the air/solution interface by touching vertically to the surface of the electrochemical solution, while another side was in contact with air as seen in Fig. 1. In this electrochemical setup, GO paper, Pt wire, and Ag/AgCl (sat. KCl) were contacted to a potentiostat as working, auxiliary, and reference electrodes, respectively. Electrochemical reduction of one side of GO paper was performed by optimization of paper thickness, electroreduction potential, reduction time, buffer concentration, and pH parameters. It is observed from Fig. 1 that the color of the electrochemically-reduced side revealed dark indigo, while the GO side is dark gray. In order to compare the efficiency of electrochemical reduction, we have prepared rGO paper by chemical reduction of GO paper by immersing it into 15 mL of 7.6 mol.L^{-1} hydriodic acid (HI) solution and leaving it in a dark place for 1 h. The paper was immersed into ethanol for three days by changing solvent many times and ultrasonically treating for 3 min at each solvent renewal till the removal of the yellow color of the solution. Finally, this paper was rinsed with distilled water and dried under open-air conditions. The electrochemically and chemically reduced rGO papers were quoted as rGO paper (er) and rGO paper (cr), respectively.

To quantitatively determine the moisture-related mechanical motion behavior of Janus GO/rGO paper, it was cut in 2 mm × 30 mm dimension and exposed to controlled humidity while recording with a digital camera. The horizontal angle of the Janus GO/rGO paper in the initial position was taken as 0° and response time and bending angle of the actuator were determined with a stopwatch and a protractor, respectively. In this experiment, we used circularly-oriented bending angle (CBA) value due to the circular movement of Janus GO/rGO paper under

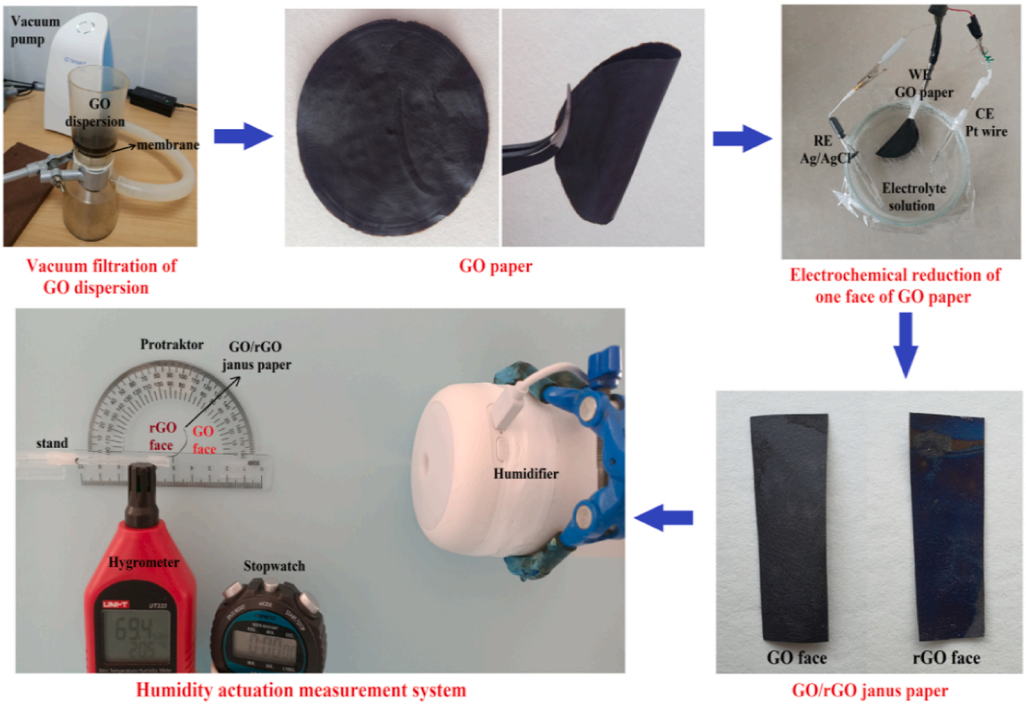

Fig. 1. Fabrication procedure and humidity actuator setup of the Janus GO/rGO paper.

moisture effect. All of the humidity actuation experiments were carried out at room temperature and open-air conditions of the laboratory. Time of the stopwatch was started and then moisture flow was provided from the humidifier to the actuator. Time reset was applied according to the starting time of the moisture flow. Throughout the study, the GO side of the actuator was positioned downwards and the rGO side upwards as illustrated in Fig. 1. The calibration curve was created by graphing the relative humidity (RH%) value in relation to the logCBA, and the response time were determined by graphing the RH% against the bending time. The repeatability and stability was also determined.

Cyclic voltammetry (CV) and chronoamperometry (CA) experiments have been applied using the Gamry brand potentiostat system. UV-Vis. absorption investigation of dispersions was collected by a Shimadzu brand spectrophotometer. Fourier transform infrared (FTIR) absorption of the paper materials was analyzed with a Perkin-Elmer spectrophotometer using specular reflectance mode attachment. Raman spectra were collected using a Witec alpha micro-Raman instrument. X-ray diffraction (XRD) patterns were provided with a Rigaku brand X-ray diffractometer (Cu-K_α, $\lambda = 1.54$ Å). Morphological analysis of the paper samples was supplied using a Zeiss Sigma 300 Scanning Electron Microscopy (SEM) system. Elemental analysis was performed using a SPECS EA 300 X-ray photoelectron (XPS) spectrometer. Surface-wetting characterization of the paper-like samples was applied using contact-angle measurements with an Attension Theta Flex instrument.

3. Results and discussion

3.1. Characterization of GO sheets

SEM images of GO and rGO (cr) layers have been illustrated in Fig. S1. Both GO and rGO (cr) layers reflect the characteristic curved surface appearance of graphene flakes [8,9]. This type of appearance reflects the flexibility and mechanical strength of the layers. It is seen that rGO (cr) sheets exhibit a more intensely curved image than GO flakes. This is an indication that the GO layers are effectively reduced by HI treatment, in which the oxygen-containing groups such as epoxy, carbonyl, hydroxyl were removed, and thus a structural change occurred. UV-Vis. absorption spectrum of the aqueous dispersion of the synthesized GO layers demonstrates the main band at about 230 nm, as well as a shoulder structure at about 300 nm (Fig. S2). The main band indicates π-π transitions originating from C═C bonds in the GO structure, and the shoulder arises due to n-π transitions from oxygen-containing functional groups [3]. For rGO (cr) layers, the π-π transition occurs at about 300 nm and the n-π transition cannot be observed clearly (Fig. S2). Hence, these two events are indications that reduction is occurring effectively.

3.2. Optimization of direct electrochemical reduction of GO paper

To determine the best conditions for one-step electrochemical reduction of GO paper, electrochemical activity was taken into consideration as a criterion. A CV experiment was conducted using a reversible redox probe of ferricyanide. CV data of GO paper in a solution containing 1.0 mM $K_3Fe(CN)_6$ and 0.1 M KNO_3 have been displayed in Fig. S3. A significant redox peak cannot be obtained and there is an IR drop for GO paper because of its highly insulating behavior. The formation of an operative and reversible redox peak pair is expected in the CV data with the increase in the reduction efficiency of GO paper.

The pH value of the solution in the electrochemical cell was initially optimized as shown in Fig. 2a. For this purpose, rGO papers (er) were prepared by electroreduction at −2.00 V in 0.10 M phosphate buffer solutions (PBS) with different pH values and their CV data was taken in a solution containing 1.0 mM $K_3Fe(CN)_6$ and 0.10 M KNO_3. No significant redox peaks were obtained for the pH 2.0–11.0 range and a peak pair emerged at pH: 12.0.

The intensity of this peak pair has also diminished at pH: 13.0. For the peak pair obtained at pH: 12.0, the potential difference between the anodic peak and the cathodic peak (ΔE_p) was calculated to be 636 mV. This value is quite high for the reversible redox process. According to this data, the most suitable pH value was considered to be 12.0. To evaluate the most suitable PBS solution concentration, rGO papers (er) were prepared by electrochemical reduction at −2.00 V for 2 h in PBS (pH: 12.0) with different concentrations. CV data of these rGO papers (er) displays reversible peak pairs for all of the studied concentrations (Fig. 2b). Considering the lowest ΔE_p as an indicator of electrochemical activity, it can be concluded that the optimum PBS concentration is 0.50 M with $\Delta E_p = 262$ mV. For the optimization of the electroreduction potential, rGO papers (er) were prepared in 0.50 M PBS (pH: 12.0) by electroreduction for 2 h at different potentials. As seen in Fig. 2c, the CVs of the papers induce that the electroreduction efficiency is very low at −1.50 V due to the absence of redox peaks. Although redox peaks occur at more negative potentials, it was determined that the lowest ΔE_p was obtained as 178 mV for −2.25 mV. Hence, this value was used as the optimum electroreduction potential. Different electrochemical reduction times were questioned as presented in Fig. 2d. It is assessed that 2 h of electroreduction is sufficient. It is supposed that the longer periods than 2 h supply mechanical fragility in the paper structure and electrochemical activity losses due to excessive reduction, while periods of less than 2 h do not provide effective reduction.

In the light of the optimization studies, rGO paper (er) was prepared by CA technique at −2.25 mV in 0.50 M PBS (pH: 12.0) for 2 h and the current-time (i-t) data obtained for this paper was demonstrated in Fig. 3a. The current is very close to 0.0 A at the beginning of the electrolysis due to insulating character of GO paper. It is observed that the current increases by time depending on the acquired conductivity of GO paper with electrochemical reduction. The decrease in the current after 25 min can be an indication of electroreduction of the inner parts with diffusion after the reduction of the GO layers on the surface.

To compare the electrochemical properties of rGO paper (er) prepared under optimum conditions, rGO paper (cr) was prepared and studied by CV experiments. In Fig. 3b, it is observed again that GO paper does not present an electrochemical activity and both rGO papers manifest reversible peak pairs. The ΔE_p values of rGO paper (er) and rGO paper (cr) were calculated as 178 mV and 172 mV, respectively. This result indicates that rGO paper (er) exhibits a close character to rGO paper (cr) in terms of electrochemical activity, which can be suitable for hydrophobic face of the Janus humidity actuator.

3.3. Characterization of Janus GO/rGO paper

The characterization of rGO paper (er) prepared under optimum conditions was examined by comparing it with rGO (cr) using different techniques. Fig. 4a displays the acquired FTIR specular reflectance spectra for GO paper, rGO paper (er), and rGO paper (cr). The most significant difference between the papers occurs in the range of 3000–3500 cm^{-1} for the –OH group. The band intensity decreases somewhat with the electrochemical reduction of GO paper containing high –OH groups. For the rGO (cr) paper, it can be evaluated that –OH groups are relatively less. At this point, it can be argued that partial reduction of GO paper is achieved by the performed electroreduction process for rGO paper (er) when compared to rGO paper (cr).

Raman spectrum of GO paper indicates the characteristic D and G bands observed at 1360 and 1590 cm^{-1}, respectively (Fig. 4b). The D band appears in defective carbon nanomaterials, and the peak intensity increases with the rise of the defect density. The G band is the vibration mode for the resulting plane for C═C bonds [18]. By considering the intensity ratios of the D and G bands (I_D/I_G), the defect densities in the structures can be evaluated [3,18]. The I_D/I_G values were calculated as 0.9, 1.0, and 1.6 for GO paper, rGO paper (er), and rGO paper (cr), respectively. It is clear from these results that the most efficient reduction occurred for rGO paper (cr). Thus, it is confirmed that rGO paper (er) undergoes partial reduction. A band group occurs at approximately

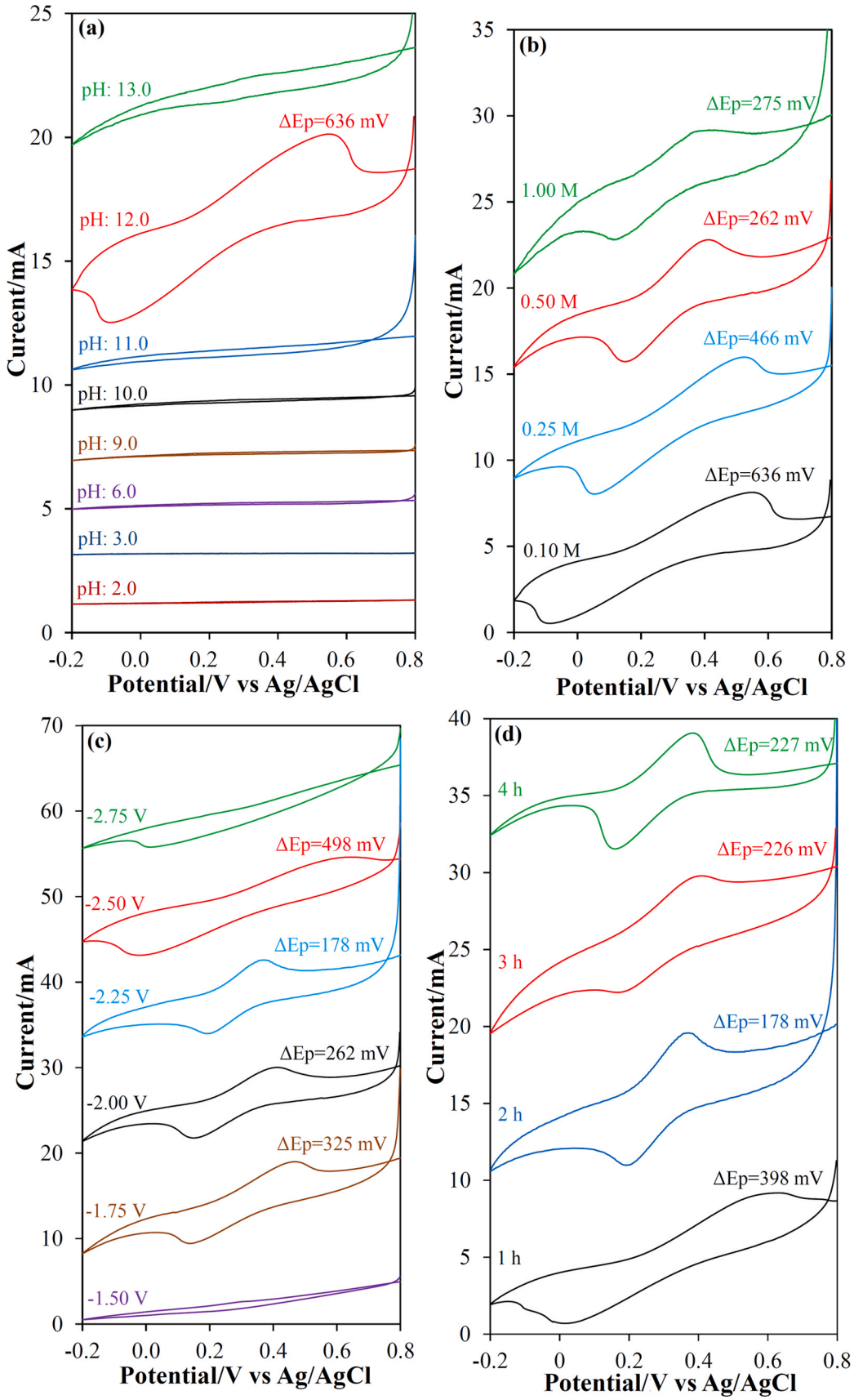

Fig. 2. CV data of rGO papers for $Fe(CN)_6^{3-}$ probe prepared a) at different pHs applying −2.00 V for 2 h in 0.10 M PBS, b) at different concentration of PBS (pH: 12.0) applying − 2.00 V for 2 h, c) at different electroreduction potentials for 2 h in 0.50 M PBS (pH: 12.0), d) at different electroreduction times at −2.25 V in 0.50 M PBS (pH: 12.0). Scan rate: 5 $mV.s^{-1}$.

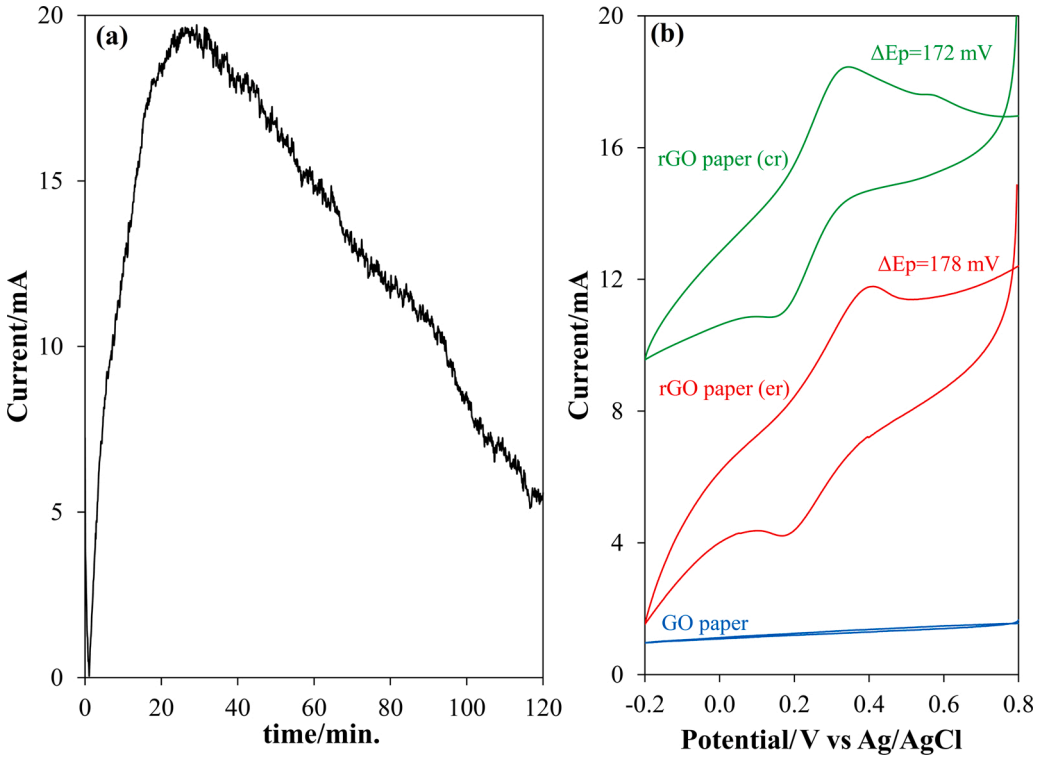

Fig. 3. a) I-t curve of CA application for electrochemical reduction of GO paper at − 2.25 V for 2 h in 0.50 M PBS (pH: 12.0), b) CV data of different paper samples for $Fe(CN)_6^{3-}$ probe. Scan rate: 5 $mV.s^{-1}$.

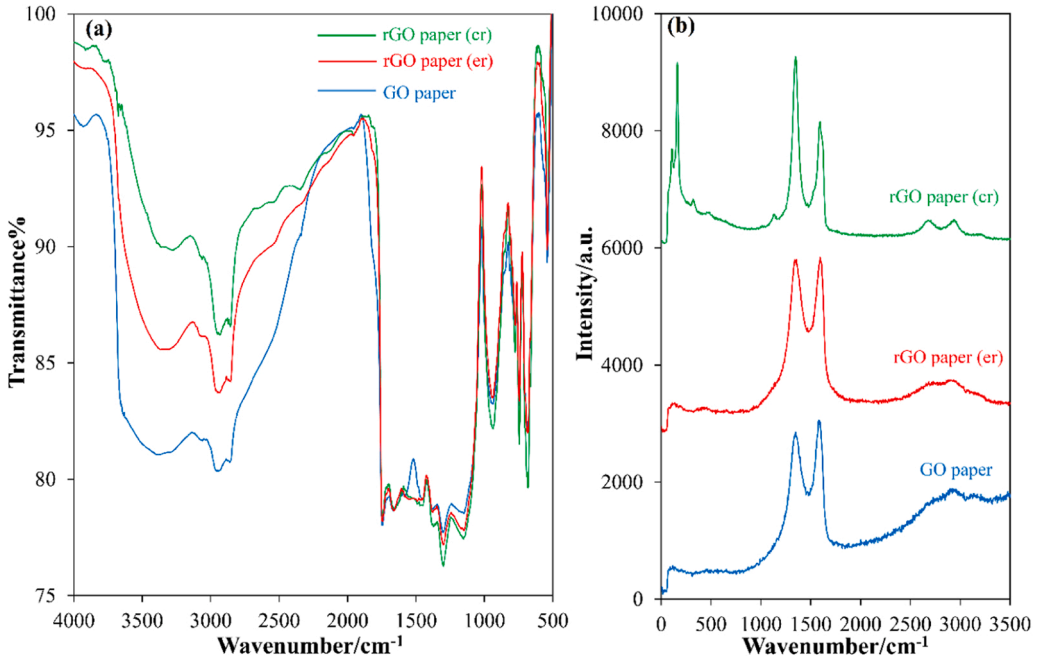

Fig. 4. FTIR specular reflectance (a) and Raman (b) spectra of various paper samples.

170 cm^{-1} in the Raman spectrum of rGO paper (cr) are indicative of iodine [37,38], which is doped to the structure as an impurity during chemical reduction of GO paper.

Since graphene is a carbon-based nanomaterial and is produced by exfoliation of graphite, it should be noted that the main peak for graphite arises around 2θ= 26.4° for 002 diffraction in XRD analysis (ICDD-PDF # 411487) [39]. For this peak, the distance between layers (d) corresponds to 0.34 nm. A peak of 2θ= 12.4° was observed for GO paper (d=0.72 nm), indicating that the interlayer distance was expanded due to the chemical oxidation process (Fig. 5a). The reason for this widening is the addition of oxygen-containing functional groups between the layers by the performed oxidation process. The XRD spectrum of rGO paper (cr) manifests a peak at 2θ= 24.6° (d=0.36 nm) while rGO paper (er) representing it at 2θ= 21.0° (d=0.42 nm), indicating that both chemical and electrochemical approaches provide reduction of GO paper. Partial reduction for rGO paper (er) can be deduced from XRD

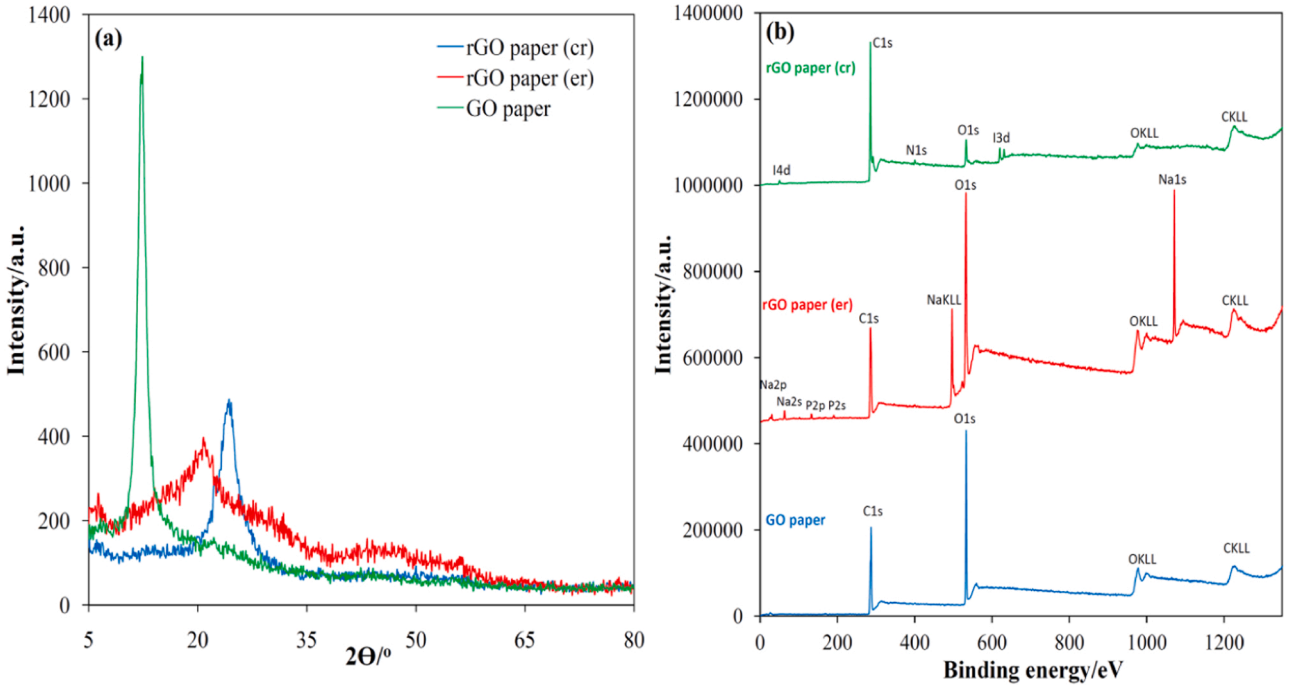

Fig. 5. Powder XRD (a) and survey scan XPS data (b) of different paper samples.

investigation due to relatively wider d distance when compared to that of rGO paper (cr).

For detailed information about the chemical compositions of the paper samples, XPS analyses have been applied as seen in Fig. 5b and Table S1. The GO paper contains a high level of C and O elements as well as a very low amount of S (0.27%). Sulfur is estimated to be an impurity from the concentrated sulfuric acid used during the oxidation of graphite. The rGO paper (cr) includes C and O elements besides small amounts of N and I. It can be stated that nitrogen is added to the structure from air and iodine comes from HI used in the reduction process. In the rGO paper (er) structure, C and O are observed from the graphitic structure as expected. A low amount of S and N elements are assigned to the usage of sulfuric acid and nitrogen from the air, respectively. The Na and P in the structure are probably due to the high amount of NaOH and Na_3PO_4 salt present in the basic solution of the electrochemical cell. It is noteworthy that the rGO paper(er) structure has higher oxygen content than rGO paper (cr). This can be attributed to the doping of phosphate and hydroxyl ions between the layers during electrochemical reduction from the basic medium.

Regional XPS spectra of rGO papers have been analyzed by deconvolution process (Figs. S4 and S5). The GO paper contains intensive C—O and C═O bonds besides a relatively low levels of C—C and C═C bonds, while the intensity of C—O and C═O diminishes and C—C and C═C bonds rise for rGO paper (cr). This case shows effective chemical reduction of GO paper. In the case of rGO paper (er), C—O and C═O bonds are higher than that of rGO paper (cr) and lower than that of GO paper, confirming the partial reduction. As seen in Fig. S5, the presence of the P—O bond in the rGO paper (er) structure as well as the C—O bond confirms the intercalation of phosphate species during electrochemical reduction. It is estimated from the Na region analysis in Fig. S5 that the sodium species doped to the rGO paper (er) structure are in ionic form.

SEM analyzes were performed to provide morphological information about the prepared paper samples. Fig. 6a reveals the surface image of the GO paper. The presence of the curled structure in the paper structure draws attention as in the GO layers depicted in Fig. S1. A high magnification view of the GO paper surface reveals a homogeneous structure and details of the folds are visible (Fig. 6b). When one side of GO paper is electrochemically reduced under optimum conditions, the small folds on the surface increase as represented in Fig. 6d and e. Fig. 6g and h indicate that the curl density for rGO paper (cr) is higher than for other papers. This case also verifies the partial reduction of GO paper after performed a one-step electroreduction process. To assess the packing properties of the rGO paper after reduction approaches, a cross-sectional SEM investigation was also performed as displayed in Fig. 6. It is monitored that regularly stacked GO sheets are organized by the applied vacuum effect (Fig. 6c). The mean paper thickness of GO paper is measured as 29.9 μm.

For the rGO paper (cr) sample (Fig. 6i), the thickness is approximately 29.6 μm, the layer-by-layer organization is protected, and the layer edges are observed more clearly compared to the GO paper. This case shows that oxygen-containing functional groups are eliminated from the GO paper structure after the chemical reduction process and the spaces between layers do not league together which may be due to doping the paper structure with iodine species. As noted before, the GO paper structure is quite insulating and this situation can result in relatively low SEM image quality (Fig. 6c). This case supplies an advantage to discriminate reduced and unreduced parts of the Janus paper. The electrochemically reduced (upside) and unreduced (downside) parts of the Janus GO/rGO paper sample are observed in Fig. 6f and Fig. S6. The mean thickness of this paper is calculated as 33.8 μm, indicating higher expansion after electrochemical reduction due to a high degree of doping with both phosphate and hydroxyl ions during one-step electrochemical reduction.

For the humidity actuator application, the GO side of Janus GO/rGO paper must be hydrophilic and the rGO side is expected to be relatively hydrophobic. To determine these features, water contact angle measurements were carried and the results are illustrated in Fig. 6j-l. Mean water contact angles for GO paper, rGO paper (er), and rGO paper (cr) were determined as 33.5°, 42.1°, and 66.6° respectively. GO paper is the most hydrophilic, and rGO paper (cr) has the most hydrophobic structure. The rGO paper (er) exhibits a relatively low hydrophobic character compared to rGO paper (cr) but it has more hydrophobicity than GO paper due to the partial reduction. Compared to GO paper, rGO paper (er) was evaluated to be relatively hydrophobic and testable for moisture actuator studies.

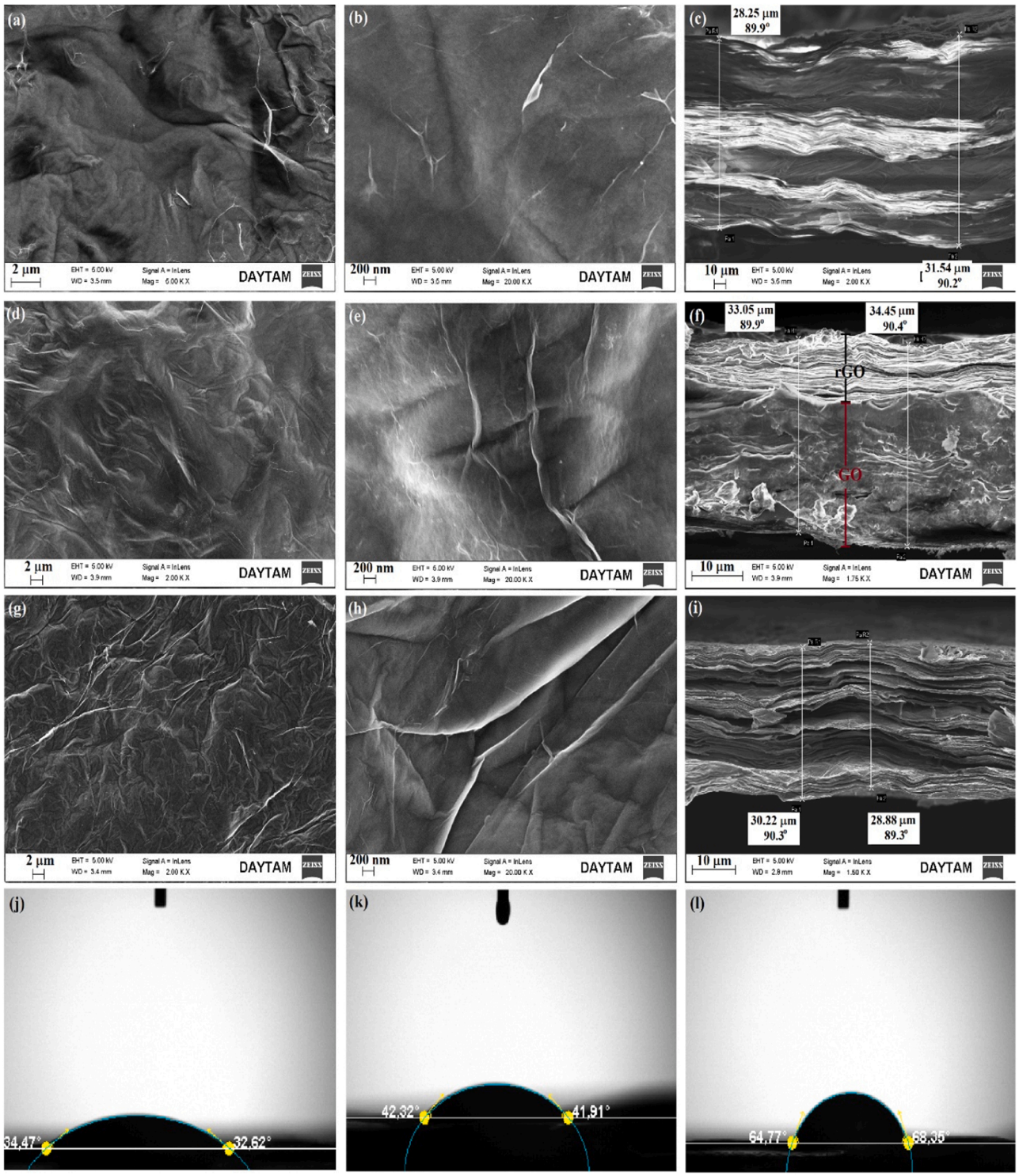

Fig. 6. Surface (a,b,d,e,g,h) and cross-sectional (c,f,i) SEM images of GO paper (a-c), GO/rGOJanus paper (d-f), and rGO (cr) paper (g-i).Contact angle measurement of GO paper (j), rGO (er) paper (k), and rGO (cr) paper (l).

3.4. Humidity actuator performance of Janus GO/rGO paper

The general view of the study designed for the actuator behavior of the Janus GO/rGO paper is shown in Fig. 7. It is observed that the actuator which is fixed horizontally and flatly at the 0° value of the protractor exhibits a circular motion when exposed to moisture and takes an almost circular form by the moisture. In this experimental setup, it was also found that the circular shape returns to its initial flat position when the moisture is interrupted (Video S1). It can be proposed that the rGO surface repels water molecules due to its hydrophobic character while the hydrophilic GO side swells till surface saturation with water molecules. This case produces stress from the GO side to the rGO surface and results in a circular folding. In the case of interruption of humidity, water molecules are desorbed from the GO surface and the Janus paper turns into a straight position again.

Supplementary material related to this article can be found online at doi:10.1016/j.snb.2021.131198.

The actuator can make bending and opening movements in

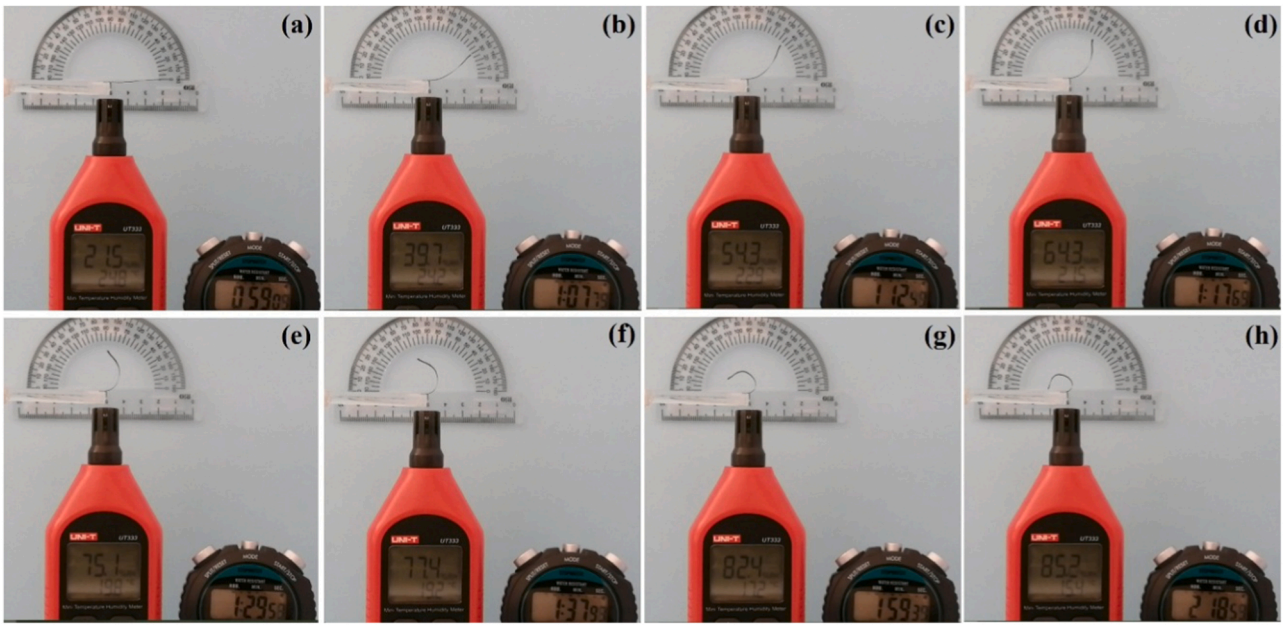

Fig. 7. Humidity actuator experiment for Janus GO/rGO paper.

proportion to the amount of moisture. It has been determined from the average of 10 experiments that the logarithm of the CBA value for this angular movement has a linear relationship with the RH% (Fig. 8a). Evaluating the humidity actuator results in Fig. 7, elapsed times for the actuator to bend forward (with moisture flow) and backward (after moisture interruption) are plotted against CBA (Fig. 8b and c). The act of the actuator is repeatable in both directions and the forward response time is relatively longer than the backward time at all bending angles. For an example, while the actuator reaches 300° in 68 s in its forward movement, it takes 53 s to move back to 0°. We have also tested GO/rGO paper (cr) by the same experimental protocol and the actuator arrived from 0° to 300° in 21 s while back action is completed in 18 s. This case can be attributed to the effective reduction of GO paper by chemical reduction process. However, the chemical reduction process by HI requires the usage of many hazardous reagents and it takes a very long time (around three days) to prepare Janus GO/rGO structure. The performed one-pot electrochemical reduction process can be handled in approximately 2 h and electrochemistry is an environmentally-friendly technique.

The thickness of GO/rGO paper is an important issue for moisture actuator performance. To evaluate the thickness effect, additional GO papers were prepared by vacuum filtration of 80 and 120 mL GO dispersions. The GO/rGO papers were formed by electrochemical reduction of one side under optimum conditions, and then their actuation against moisture was questioned (Fig. S7). These actuators were quoted as GO/rGO-80 paper and GO/rGO-120 paper, respectively. For GO/rGO-80 paper, a bending motion from CBA= 0° to a maximum CBA of approximately 170° could be obtained at RH%= 83.1, and the duration of this motion was 117 s (Fig. S7a and b). The bending motion of GO/rGO-120 paper can be obtained from CBA= 0° to the highest CBA of 40° at RH %= 84.9 in 111 s (Fig. S7c and d). These quality values appear to be very low when compared to the results of the actuator prepared by vacuum

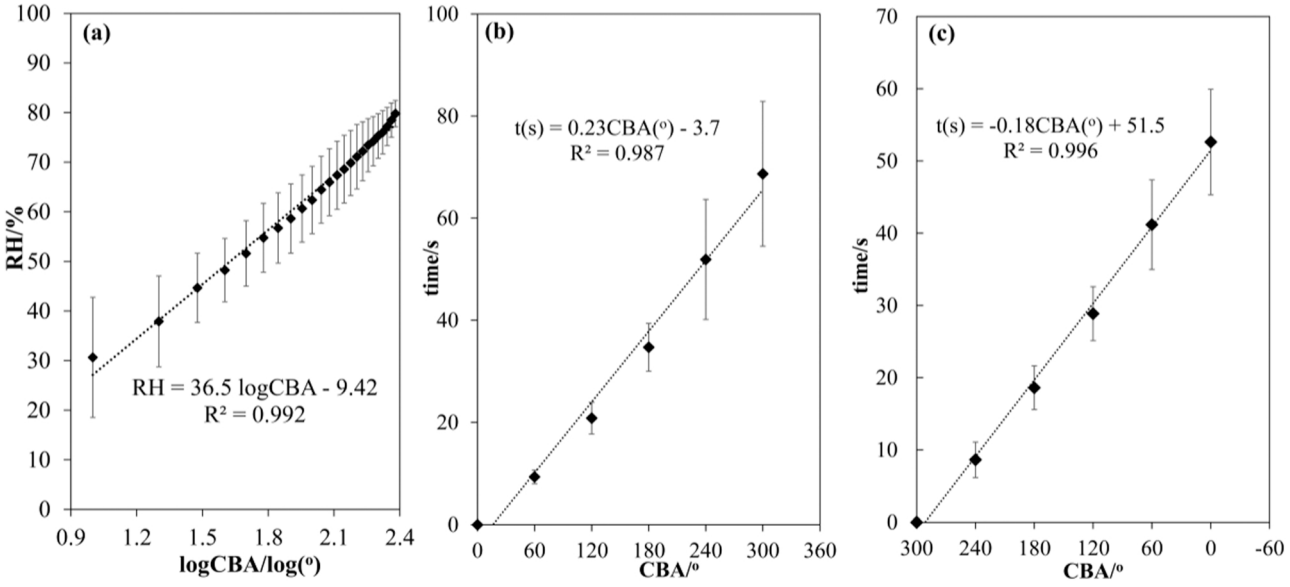

Fig. 8. The dependency between (a) RH% and logCBA (calibration curve). The dependency between response time and bending angle for forward (b) and reverse (c) movement of Janus GO/rGO actuator (n = 10).

filtration of 100 mL GO dispersion (Figs. 7 and 8). Thus, the most suitable paper thickness is decided as approximately 34 μm (Fig. 6f). It can be proposed that the flexibility decreases in thicker paper structures. In the formation of thinner paper, it is estimated that the bending performance decreases with the decrease in the hydrophilic GO layer when the thickness of the electrochemically reduced layer is taken into account.

To test the production reproducibility of Janus GO/rGO paper for moisture actuator studies, 3 different actuators were manufactured using the same fabrication method. Elapsed time for each paper to reach CBA= 180° was determined (Fig. S8a) and the relative standard deviation (RSD) value was determined as 5.3%, indicating the quite repeatable production of GO/rGO paper for humidity actuator application. We have also examined the time-dependent stability of Janus GO/rGO paper by measuring elapsed time to reach CBA= 180° at certain time intervals during 60 days. The actuator was left in the laboratory conditions in a clean place, when not used. As displayed in Fig. S8b, the bending time was plotted against the holding time and no significant variation was observed depending on holding time with an RSD of 6.0%. The successive usage stability of the actuator was studied and response time to achieve CBA of 60, 120, and 180° values were measured for 30 repetitive moisture dependent actions as illustrated in Fig. S9. It is observed that no regular increase at response time was observed for all studied angles. The sequential actions resulted in fluctuation of response time and RSD values of 1.4, 2.8, and 4.3 were calculated for CBA of 60, 120, and 180° respectively, indicating a good repeatability of the actuator.

To show the usability of this Janus GO/rGO paper in technological applications, we have designated a four-fingered claw system using Janus GO/rGO papers as a finger (Video S2). We have observed that the claw model can grasp a sponge by moisture effect and leaves it after interruption of the humidity. It was also shown that the straight shape of GO/rGO paper transforms into a circle suddenly when soaked into water (Video S3). These abilities flash the usage possibility of Janus GO/rGO paper for artificial muscles.

Supplementary material related to this article can be found online at doi:10.1016/j.snb.2021.131198.

4. Conclusions

GO paper structure has been altered to rGO character using one-step electrochemical reduction under optimized conditions. CV experiment for ferricyanide probe indicated that the produced rGO paper (er) has a very close electrochemical activity to rGO paper (cr). Reduction efficiency of electrochemical reduction outcomes partially reduced structure based on FTIR, Raman, XPS, XRD, and water contact angle analyses, when compared to that of rGO paper (cr). Morphological investigations in terms of cross-sectional SEM analysis exhibited that one side of GO paper was effectively reduced after the one-step electroreduction route under optimized conditions. This Janus GO/rGO design circularly moved under moisture, in which a relationship between RH% and logCBA was achieved. Humidity actuation experiments revealed high stability of the Janus GO/rGO paper and reproducibility of the proposed method for humidity actuator tests. This actuator system can be a useful material for the design of hygrometers and artificial muscles. It can be concluded that the reduction efficiency of the proposed electrochemical route need to be developed because its moisture dependent response time is almost two times higher than that of chemical reduction with HI. However, the chemical reduction demands hazardous chemicals and its application takes approximately 3 days. The one-pot electrochemical reduction, an environmentally-friendly approach, is completed in a very short time of 2 h.

CRediT authorship contribution statement

Zeriş Aksu: Investigation, Data curation, Methodology. **Cengiz Han Şahin:** Investigation. **Murat Alanyalıoğlu**: Project administration, Conceptualization, Writing – review & editing, Supervision.

Declaration of Competing Interest

The authors declare that they have no known competing financial interests or personal relationships that could have appeared to influence the work reported in this paper.

Acknowledgements

This study was supported by the Scientific and Technological Research Council of Turkey (TÜBİTAK) under project no: 120Z155. C. H.Ş. thanks the STAR scholarship program of TÜBİTAK.

Appendix A. Supporting information

Supplementary data associated with this article can be found in the online version at doi:10.1016/j.snb.2021.131198.

References

[1] K.S. Novoselov, A.K. Geim, S.V. Morozov, D. Jiang, Y. Zhang, S.V. Dubonos, I. V. Grigorieva, A.A. Firsov, Electric field effect in atomically thin carbon films, Science 306 (2004) 666–669.
[2] R.A. Gaashani, A. Najjar, Y. Zakaria, S. Mansour, M.A. Atieh, XPS and structural studies of high quality graphene oxide and reduced graphene oxide prepared by different chemical oxidation methods, Ceram. Int. 45 (2019) 14439–14448.
[3] M. Alanyalıoğlu, J.J. Segura, J. Oro-Sole, N. Casan-Pastor, The synthesis of graphene sheets with controlled thickness and order using surfactant-assisted electrochemical processes, Carbon 50 (2012) 142–152.
[4] A. Özturk, M. Alanyalıoğlu, Electrochemical fabrication and amperometric sensor application of graphene sheets, Superlattices Microstruct. 95 (2016) 56–64.
[5] B. Deng, Z. Liu, H. Peng, Toward mass production of CVD graphene films, Adv. Mater. 31 (2019), 1800996.
[6] T. Beyazay, F.E.S. Öztuna, U. Ünal, Self-standing reduced graphene oxide papers electrodeposited with manganese oxide nanostructures as electrodes for electrochemical capacitors, Electrochim. Acta 296 (2019) 916–924.
[7] H. Gürsu, M. Gençten, Y. Şahin, Preparation of N-doped graphene-based electrode via electrochemical method and its application in vanadium redox flow battery, Int. J. Energy Res. 42 (2018) 3851–3860.
[8] K. Dağcı, M. Alanyalıoğlu, Preparation of free-standing and flexible graphene/Ag nanoparticles/poly(pyronin Y) hybrid paper electrode for amperometric determination of nitrite, ACS Appl. Mater. Interfaces 8 (2016) 2713–2722.
[9] E. Topçu, E, K. Dağcı, M. Alanyalıoğlu, Free-standing graphene/poly(methylene blue)/AgNPs composite paper for electrochemical sensing of NADH, Electroanalysis 28 (2016) 2058–2069.
[10] S. Park, J. An, J.W. Suk, R.S. Ruoff, Graphene-based actuators, Small 6 (2010) 210–212.
[11] M. Sun, J. Li, Graphene oxide membranes: functional structures, preparation and environmental applications, Nanotoday 20 (2018) 121–137.
[12] E. Erçarıkcı, M. Alanyalıoğlu, Dual-functional graphene-based flexible material for membrane filtration and electrochemical sensing of heavy metal ions, IEEE Sens. J. 21 (2021) 2468–2475.
[13] Y.Q. Liu, J.N. Ma, Y. Liu, D.D. Han, H.B. Jiang, J.W. Mao, C.H. Han, Z.Z. Jiao, Y. L. Zhang, Facile fabrication of moisture responsive graphene actuators by moderate flash reduction of graphene oxides films, Opt. Mater. Express 7 (2017) 2617–2625.
[14] D. Sun, X. Yan, J. Lang, Q.W. Xue, High performance supercapacitor electrode based on graphene paper via flame-induced reduction of graphene oxide paper, J. Power Sources 222 (2013) 52–58.
[15] Z. Bo, W. Zhu, X. Tu, Y. Yang, S. Mao, Y. He, J. Chen, J. Yan, K. Cen, Instantaneous reduction of graphene oxide paper for supercapacitor electrodes with unimpeded liquid permeation, J. Phys. Chem. C 118 (2014) 13493–13502.
[16] S. Liu, K. Chen, Y. Fu, S. Yu, Z. Bao, Reduced graphene oxide paper by supercritical ethanol treatment and its electrochemical properties, Appl. Surf. Sci. 258 (2012) 5299–5303.
[17] H. Chen, Z. Song, X. Zhao, X. Li, H. Lin, Reduction of free-standing graphene oxide papers by a hydrothermal process at the solid/gas interface, RSC Adv. 3 (2013) 2971–2978.
[18] G.K. Ramesha, S. Sampath, Electrochemical reduction of oriented graphene oxide films: an in situ raman spectroelectrochemical study, J. Phys. Chem. C. 113 (2009) 7985–7989.
[19] X.Y. Peng, X.X. Liu, D. Diamond, K.T. Lau, Synthesis of electrochemically-reduced graphene oxide film with controllable size and thickness and its use in supercapacitor, Carbon 49 (2011) 3488–3496.
[20] H.O. Doğan, D. Ekinci, Ü. Demir, Atomic scale imaging and spectroscopic characterization of electrochemically reduced graphene oxide, Surf. Sci. 611 (2013) 54–59.
[21] J. Kauppila, J.P. Kunnas, P. Damlin, A. Viinikanoja, C. Kvarnström, Electrochemical reduction of graphene oxide films in aqueous and organic solutions, Electrochim. Acta 89 (2013) 84–89.

[22] Y. Harima, S. Setodoi, I. Imae, K. Komaguchi, J. Ohshita, H. Mizota, J. Yano, Electrochemical reduction of graphene oxide in organic solvents, Electrochim. Acta 56 (2011) 5363–5368.
[23] E. Wang, M.Y. Desai, S.W. Lee, Light-controlled graphene-elastin composite hydrogel actuators, Nano Lett. 13 (2013) 2826–2830.
[24] H. Kim, J.H. Moon, T.J. Mun, T.G. Park, G.M. Spinks, G.G. Wallace, S.J. Kim, Thermally responsive torsional and tensile fiber actuator based on graphene oxide, ACS Appl. Mater. Interfaces 10 (23018) (2018) 32760–32764.
[25] J. Liang, L. Huang, N. Li, Y. Huang, Y. Wu, S. Fang, J. Oh, M. Kozlov, Y. Ma, F. Li, R. Baughman, Y. Chen, Electromechanical actuator with controllable motion, fast response rate, and high-frequency resonance based on graphene and polydiacetylene, ACS Nano 6 (2012) 4508–4519.
[26] Y. Qiu, M. Wang, W. Zhang, Y. Liu, Y.V. Li, K. Pan, An asymmetric graphene oxide film for developing moisture actuators, Nanoscale 10 (2018) 14060–14066.
[27] Y. Ge, R. Cao, S. Ye, Z. Chen, Z. Zhu, Y. Tu, D. Ge, X. Yang, A bio-inspired homogeneous graphene oxide actuator driven by moisture gradients, Chem. Commun. 54 (2018) 3126–3129.
[28] D.D. Han, Y.L. Zhang, H.B. Jiang, H. Xia, J. Feng, Q.D. Chen, H.L. Xu, H.B. Sun, Moisture-responsive graphene paper prepared by self-controlled photoreduction, Adv. Mater. 27 (2015) 332–338.
[29] D.D. Han, Y.L. Zhang, Y. Liu, Y.Q. Liu, H.B. Jiang, B. Han, X.Y. Fu, H. Ding, H.L. Xu, H.B. Sun, Bioinspired graphene actuators prepared by unilateral UV irradiation of graphene oxide papers, Adv. Funct. Mater. 25 (2015) 4548–4557.
[30] J.N. Ma, J.W. Mao, D.D. Han, X.Y. Fu, Y.X. Wang, Y.L. Zhang, Laser programmable patterning of RGO/GO Janus paper for multiresponsive actuators, Adv. Mater. Technol. 4 (2019), 1900554.
[31] J. Mu, C. Hou, B. Zhu, H. Wang, Y. Li, Q. Zhang, A multi-responsive water-driven actuator with instant and powerful performance for versatile applications, Sci. Rep. 5 (2015) 9503.
[32] W. Zhang, L. Wang, K. Sun, T. Luo, Z. Yu, K. Pan, Graphene-based Janus film with improved sensitive response capacity for smart actuators, Sens. Actuators B 268 (2018) 421–429.
[33] G. Xu, J. Chen, M. Zhang, G. Shi, An ultrasensitive moisture driven actuator based on small flakes of graphene oxide, Sens. Actuators B 242 (2017) 418–422.
[34] D.D. Han, Y.Q. Liu, J.N. Ma, J.W. Mao, Z.D. Chen, Y.L. Zhang, H.B. Sun, Biomimetic graphene actuators enabled by multiresponse graphene oxide paper with pretailored reduction gradient, Adv. Mater. Technol. 3 (2018), 1800258.
[35] J. Yang, J. Zhang, X. Li, J. Zhou, Y. Li, Z. Wang, J. Cheng, Q. Guan, B. Wang, Single janus iodine-doped rGO/rGO film with multi-responsive actuation and high capacitance for smart integrated electronics, Nano Energy 53 (2018) 916–925.
[36] S.Y. Lee, R.B. Moore, R.L. Mahajan, An Al-assisted GO/rGO Janus film: Fabrication and hygroscopic properties, Carbon 171 (2021) 585–596.
[37] G. Kalita, K. Wakita, M. Takahashi, M. Umeno, Iodine doping in solid precursor-based CVD growth graphene film, J. Mater. Chem. 21 (2011) 15209–15213.
[38] S. Pei, J. Zhao, J. Du, W. Ren, H.M. Cheng, Direct reduction of graphene oxide films into highly conductive and flexible graphene films by hydrohalic acids, Carbon 48 (2010) 4466–4474.
[39] Z. Aksu, M. Alanyalıoğlu, Fabrication of free-standing reduced graphene oxide composite papers doped with different dyes and comparison of their electrochemical performance for electrocatalytical oxidation of nitrite, Electrochim. Acta 258 (2017) 1376–1386.

Zeriş Aksu was born in Erzurum, Turkey in 1985. She received the B.S., and M.S. degrees in Chemistry department of Atatürk University in 2014 and 2017, respectively. She is still working as Ph. D. student in Atatürk University since 2018. Her research topics are electrochemical sensors and actuators.

Cengiz Han Şahin was born in Kars, Turkey in 1999 and he is still B.S. student in Dentistry Faculty of Atatürk University.

Murat Alanyalıoğlu was born in Balıkesir, Turkey in 1974. He received the B.S., M.S. and Ph.D. degrees in Chemistry department of Atatürk University in 1997, 2001, and 2006, respectively. He has worked on the topic of electrochemical synthesis of semiconductor thin films for 9 months in Auburn University, AL, USA between 2002 and 2003. He has performed post-doctoral studies on the electrochemical synthesis of graphene sheets for about one year at ICMAB, Barcelona, Spain. He is still working as full Professor in Bilecik Şeyh Edebali University since 2021. His research interest includes electrochemical sensors, actuators, graphene-based nanocomposites, electropolymerization, and semiconductor thin films.